J Math Chem (2013) 51:1139–1152
DOI 10.1007/s10910-012-0097-4

REVIEW

A thermal model and experimental procedure for a point-source approach to determining the thermal properties of drill cuttings

M. A. Rey-Ronco · T. Alonso-Sánchez · J. Coppen-Rodríguez · M. P. Castro-García

Received: 23 July 2012 / Accepted: 21 September 2012 / Published online: 16 October 2012

Abstract This paper discusses a new procedure for calculating the conductivity and volumetric heat capacity of drill cuttings from boreholes, an important factor when designing shallow geothermal systems. The experiment in question consists of placing 55–65 kg drill cutting samples inside a container, along with a heat source (point source assumed), and arranging temperature sensors, connected to a data logger, at known distances from the source. A mathematical method for determining the conductivity and volumetric heat capacity associated with this experiment is described.

Keywords Thermal conductivity · Volumetric heat capacity · Geothermal energy · Cuttings · Borehole

1 Introduction

While the problems inherent to the use of fossil fuels and nuclear energy have become increasingly apparent in recent years, alternative energy sources with a much lower impact on the environment are undergoing steady progress. Among them, low-enthalpy

M. A. Rey-Ronco
Departamento de Energía, Universidad de Oviedo, Oviedo 33004, Spain
e-mail: rey@uniovi.es

T. Alonso-Sánchez · J. Coppen-Rodríguez · M. P. Castro-García (✉)
Departamento de Explotación y Prospección de Minas, Universidad de Oviedo, Oviedo 33004, Spain
e-mail: castromaria@uniovi.es

T. Alonso-Ságuez
e-mail: tjalonso@uniovi.es

J. Coppen-Rodría
e-mail: coppenjonas@uniovi.es

geothermal energy is developing in exciting new directions, particularly in countries like Spain, where the geology is not suitable for high temperatures at great depths.

Shallow geothermal energy relies heavily on in situ ground thermal data in order to function properly. As such, the aim of this study is to use simple and inexpensive thermal tests, carried out with drill cuttings, in order to determine two important ground thermal properties: volumetric heat capacity and thermal conductivity. While tabulated data or measurements taken from borehole thermal response tests (TRT) are important tools, our method constitutes an appealing alternative or complement, since it provides data which are specific to each geothermal site. Once the data are collected, an original mathematical model is used to process them, providing a set of essential parameters for the design of a ground-coupled geothermal installation.

This subject has been studied by several researchers, who have focused mainly on the analysis of thermal conductivity as a basic parameter for controlling heat flow [1,2].

Other researchers have developed their own methods to estimate conductivity in sedimentary basins [3] and by testing boreholes in situ (TRT) [4–6].

Of the various existing methods for determining ground thermal properties in situ, there are two that stand out: the linear source method and the cylindrical source method, both of which offer analytical solutions to the problem of heat transmission from a source into an infinite homogeneous medium.

The linear source method is based on the traditional theory that over sufficiently long periods of time, heat exchange in the ground can be modelled as a linear heat source in an infinite medium [7,8].

In the cylindrical source method the elements that exchange heat with the ground are modelled as cylindrical heat sources in an infinite medium [8]. While Deerman and Kavanaugh [9] extended this model to variable heat flow, their method made it so that the data were difficult to analyze. Some other authors [9–12] have proposed more detailed numerical models in two and three dimensions.

In this paper we propose a simple laboratory method to determine the thermal parameters both of borehole cuttings, as well as other ground samples in the form of cuttings. This method involves heating the sample with a point heat source whose output is known, and using sensors located at known distances from the source to measure the temperatures at constant time intervals.

2 Hypothesis

In order to simplify the mathematical model as much as possible, and to be able to apply the point heat source method, we have chosen a spherical study geometry. The premises of this study are as follows:

- The sample is made up of cuttings from roto-percussion drilling, and its density and lithology are homogeneous.
- The volume of the container that holds the sample is considered to be infinite. This premise is only valid for the points inside the container that are furthest from the container's wall.

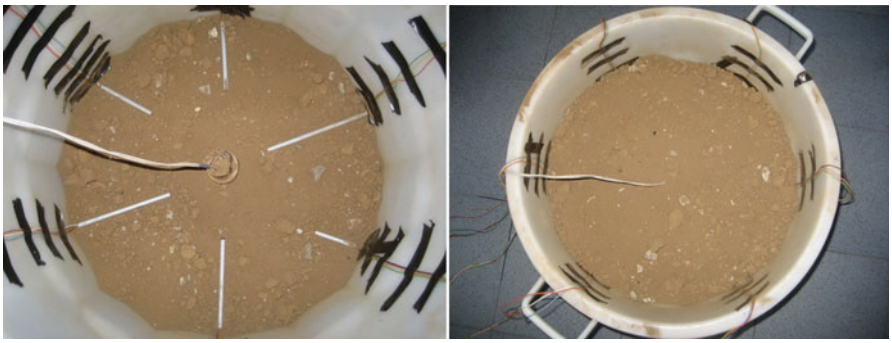

Fig. 1 Sensors before and after being covered by the ground sample

- The heat source is placed in the center of the container, is essentially spherical, and has a small diameter. Given the dimensions of the sample, the source is considered to be a point heat source. The greater the distance between the sensor and the heat source, the truer this premise becomes.
- The thermal flow is radial. This premise is sufficiently true past a certain distance away from the source, and before the wall of the container, which is cylindrical in shape.
- The heat released by the sample, the walls of the container, the top of the container, etc., follows a constant convection coefficient.
- At the moment that heating begins, all points in the sample have the same temperature.
- There is a discreet number N of temperature sensors situated on a horizontal radius at distances R_i from the center of the heat source. A sensor is placed on the external surface of the container, and another on the internal surface to monitor the ambient temperature.

3 Experimental set-up

The weight of the samples used in this laboratory method, be they borehole drill cuttings or something essentially similar, ranges from 55 to 65 kg, and are to be placed in a cylindrical container that is 45 cm tall and 48 cm in diameter.

In the centre of the cylindrical container there is a small incandescent light bulb, which we assume to be a point heat source. On the same horizontal plane as this source, and at known distances from its centre, there are six sensors located inside the sample itself, at 4.5, 5.5, 6.5, 8.5, 11 and 15 cm from the centre of the bulb, one on the exterior surface of the container, and another in the laboratory in order to evaluate the convection coefficient h (Fig. 1). Four different types of lithologies have been analyzed: clay, sand, limestone and shale, in the form of fragments or dry cuttings.

The temperature sensors are small LM35 integrated-circuit sensors, whose output voltage is proportional to the temperature in degrees Celsius. The sensors can handle temperatures of up to 150 °C, which is higher that the maximum temperatures reached when heating the samples. The sensors are connected to an ADC-16 data logger

(www.picotech.com). This data logger sends the data directly to a PC via USB, where they are treated with the corresponding software applications.

We have applied a new model, which we will refer to as "point heat source," and involves, as mentioned above, various hypotheses about the sample (infinite, homogeneous, isotropic), the heat source (point), the heat flow (radial), and the sensors (point), in order to simplify the mathematic model.

4 Thermal conductivity k

In steady-state conditions, and given the hypotheses made for this model, we can use the equation for heat flow $\phi = \frac{\mathrm{P}}{4\cdot\pi\cdot\mathrm{r}^2}$ and the Fournier equation in order to determine the relationship between the temperature increase in each sensor with respect to the temperature in reference sensor $\Delta\mathrm{T_i}$, and thermal conductivity k:

$$\Delta T_i = -\frac{P}{4\cdot\pi\cdot k}\cdot\frac{1}{R_i} + \frac{P}{4\cdot\pi\cdot k}\cdot\frac{1}{R_{ref}} \tag{1}$$

where:

- P is the power of the heat source (W)
- R_i is the distance from the heat source to any sensor (m)
- k is thermal conductivity (W/mK)
- R_{ref} is the distance from a reference sensor to the heat source (m)

This equation represents a straight line, in which the y-axis represents $\Delta\mathrm{T_i}$ (steady state conditions) for each sensor, and the x-axis represents $\frac{1}{\mathrm{R_i}}$. Conductivity can be determined based on the slope of the line $\mathrm{u} = -\frac{\mathrm{P}}{4\cdot\pi\cdot\mathrm{k_u}}$ or the intersection of the line with the y-axis $\mathrm{v} = \frac{\mathrm{P}}{4\cdot\pi\cdot\mathrm{k_v}\cdot\mathrm{R_{ref}}}$.

Figure 2 contains the experimental data, while Fig. 2a shows the temperature change in the different sensors as the sample is heated, and Fig. 2b shows $\Delta\mathrm{T_i}$ (steady state conditions) versus $\frac{1}{\mathrm{R_i}}$.

The results of the different tests are shown in Table 1, and the result of the 20 experiments carried out with the four types of samples is shown in Table 2.

The sample with the lowest conductivity is the limestone cuttings, and the highest, the sand sample. The shale and clay samples have the same conductivity, 0.45 W/mK.

5 Volumetric heat capacity ($\rho.C_p$)

One of the challenges of measuring volumetric heat capacity is that it cannot be carried out in steady-state conditions. Likewise, the computational costs involved in using the PDE (partial differential equation) would be prohibitive.

Before determining $\left(\rho\cdot\mathrm{C_p}\right)$, one must first determine k, which, as we have seen, is indeed determined in steady-state conditions. By studying, during non-steady-state conditions, the model of heat transmission through a homogeneous, isotropic and

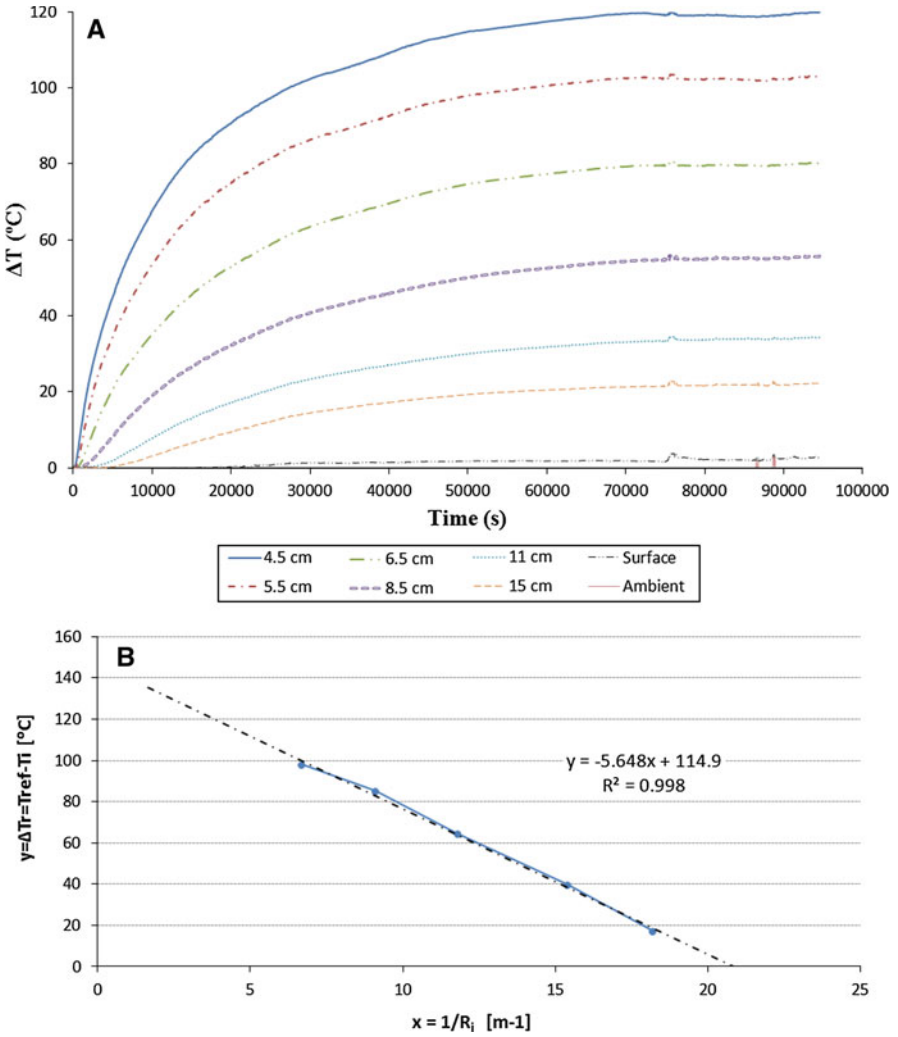

Fig. 2 Experiment data and the determination of thermal conductivity in test 5 (sand). **a** The heating process. **b** The *straight line* from Eq. 1 used to determine conductivity based on the experimental data

infinite medium, with a point heat source located at its centre, the volumetric heat capacity, ρC_p, can be found using the expression:

$$\left(\rho \cdot C_p\right) = \frac{\Delta H\,(t)}{4 \cdot \pi \cdot \int_0^{R_{ext}} T\,(r,t) \cdot r^2 \cdot dr} \tag{2}$$

where:

- H(t) is the increase in enthalpy in the system due to the presence of a point heat source.

Table 1 Thermal conductivity (k) values for the Fig. 2

Slope	$u = -\frac{P}{4\cdot\pi\cdot k_u} = -5.648$	$k_u = 0.54$
Intersection with the y-axis $\left[\mathrm{v} = \frac{\mathrm{P}}{4\cdot\pi\cdot\mathrm{k_v}\cdot\mathrm{R_{ref}}}\right]$	$v = \frac{P}{4\cdot\pi\cdot k_v\cdot R_{ref}} = 114.9$	$k_v = 0.58$

Table 2 Results of the experiments and calculations to determine k for the different dry materials in cutting form

Experiment	Clay		Sand		Limestone (detritus)		Shale (detritus)	
	k_u (W/mK)	k_v (W/mK)	k_u (W/mK)	k_v (W/mK)	k_u (W/mK)	k_v (W/mK)	k_u (W/mK)	k_v (W/mK)
1	0.44	0.47	0.57	0.59	0.41	0.43	0.44	0.47
2	0.43	0.46	0.58	0.60	0.42	0.43	0.44	0.47
3	0.44	0.47	0.58	0.60	0.41	0.42	0.44	0.44
4	0.44	0.47	0.59	0.61				
5	0.43	0.46	0.54	0.58				
6			0.54	0.58				
7			0.54	0.58				
8			0.54	0.59				
9			0.54	0.59				
Average	0.44	0.47	0.56	0.59	0.41	0.43	0.44	0.46
k	0.45		0.57		0.42		0.45	

- $T(r, t)$ is the temperature difference with respect to T_0 at a point situated at a distance r and a time t.
- T_0 is the initial temperature (°C)
- r is the distance from any point in the sample to the centre of the heat source (m)
- t is time (s)
- $\mathrm{R_{ext}}$ is the external radius of the model (m)

According to the first law of thermodynamics for an isobaric process, the increase in enthalpy in a system H (t) is equal to the heat emitted by the thermal source minus the heat lost $\mathrm{Q_p}$ (t):

$$\Delta H\,(t) = P \cdot t - Q_p(t) \tag{3}$$

The system is assumed to be a sphere with the heat source at its centre and radius $\mathrm{R_{ext}}$. The value for $\mathrm{R_{ext}}$ must satisfy the condition that the outer surface of the sphere $\mathrm{S_R}$ be the same as the surface of the cylinder that holds the sample. It is assumed that the heat transferred by conduction though the sphere, and the heat transferred by convection outside the sample, are equal. The heat lost by the system $\mathrm{Q_p}$ (t) through its external boundary, with a convection coefficient of h, is given by the expression:

$$Q_p(t) = h \cdot S_R \cdot \int_0^t T(R_{ext}, t) \cdot dt \tag{4}$$

Thus, by substituting and working out Eq. 2, we obtain:

$$(\rho C_p) = (\rho C_p)' - \frac{h \cdot S_R}{4 \cdot \pi} \cdot \frac{\int_0^t T(R_{ext}, t) \cdot dt}{\int_0^{R_{ext}} T(r, t) \cdot r^2 \cdot dr} \tag{5}$$

where:

$$(\rho C_p)' = \frac{P \cdot t}{4 \cdot \pi \cdot \int_0^{R_{ext}} T(r, t) \cdot r^2 \cdot dr} \tag{6}$$

It is assumed that the sample is large enough in size that we can disregard the error caused by the fact that the medium is not actually infinite. With the temperature sensors i it is possible to determine the temperature values at the points at distance R_i from the centre of the heat source. The points situated between two sensors i and $i+1$ are taken to have a temperature of T_{it}, which varies linearly with the distance between these two sensors. In light of all of this, Eq. 6 can be approximated as:

$$(\rho C_p)' \cong \frac{P \cdot t}{\sum_{i=1}^{N} \left[\int_{R_i}^{R_{i+1}} T_{it} \cdot dV \right]} = (\rho C_p)^* \tag{7}$$

where, $dV = 4 \cdot \pi \cdot r^2 \cdot dr$, and the interpolated value of T_{it} is:

$$T_{it} = \frac{T_{i+1,t} - T_{i,t}}{R_{i+1} - R_i} \cdot r + \left[T_{i+1,t} - \frac{T_{i+1,t} - T_{i,t}}{R_{i+1} - R_i} \cdot R_{i+1} \right]$$

Which we can work out to get:

$$(\rho C_p)^* = \frac{P \cdot t}{4 \cdot \pi \cdot \sum_{i=1}^{N} \left[\frac{b_i}{4 \cdot c_i} \cdot (T_{i+1,t} - T_{i,t}) + \frac{a_i}{3 \cdot c_i} \cdot (T_{i,t} \cdot R_{i+1} - T_{i+1,t} \cdot R_i) \right]} \tag{8}$$

where:

$$\begin{aligned} a_i &= R_{i+1}^3 - R_i^3 \\ b_i &= R_{i+1}^4 - R_i^4 \\ c_i &= R_{i+1} - R_i \end{aligned}$$

Figure 3 indicates the arrangement of the sensors and the temperature at a point at distance r, located between sensors i and $i+1$, where the temperatures at the latter two sensors are known.

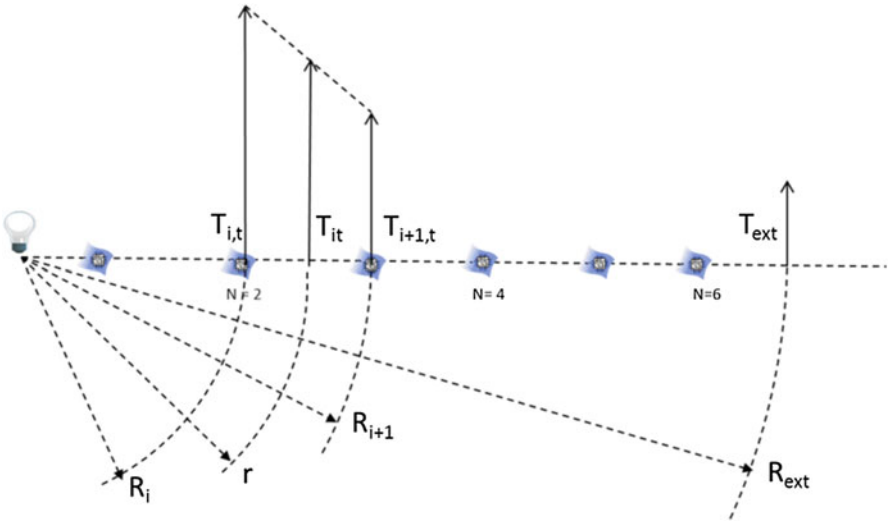

Fig. 3 General arrangement of the sensors, and determining the temperature at distance r from the heat source

According to Ingersoll et al. 1954, the temperature in a point source at any point T (r, t) that appears in the denominator of the second term in Eq. 5 can be found in terms of time and the distance from the point source by:

$$T\,(r,t) = \frac{\dot{Q}}{2\cdot\pi^{3/2}\cdot r\cdot k}\int_{r\cdot\eta}^{\infty} e^{-\beta^2}\cdot d\beta \tag{9}$$

Which can also be expressed as:

$$T\,(r,t) = \frac{\dot{Q}}{4\cdot\pi\cdot r\cdot k}\cdot(1-erf\,(x)) \tag{10}$$

where:

- $\dot{Q}$ is the heat injection rate (W)
- $x = \frac{r}{2\cdot\sqrt{\alpha\cdot t}}$
- $\alpha = \frac{\mathrm{k}}{(\rho \mathrm{C_p})}$ is thermal diffusivity (m/s^2) and,
- *erf*(x) is the complementary error function which may be expressed as:

$$erf\,(x) = \frac{2}{\sqrt{\pi}}\cdot\sum_{n=0}^{\infty}\frac{(-1)^n\cdot x^{2*n+1}}{n!\cdot(2\cdot n+1)} = \frac{2}{\sqrt{\pi}}\left(x-\frac{x^3}{3}+\frac{x^5}{10}-\frac{x^7}{42}+\frac{x^9}{216}-\cdots\right) \tag{11}$$

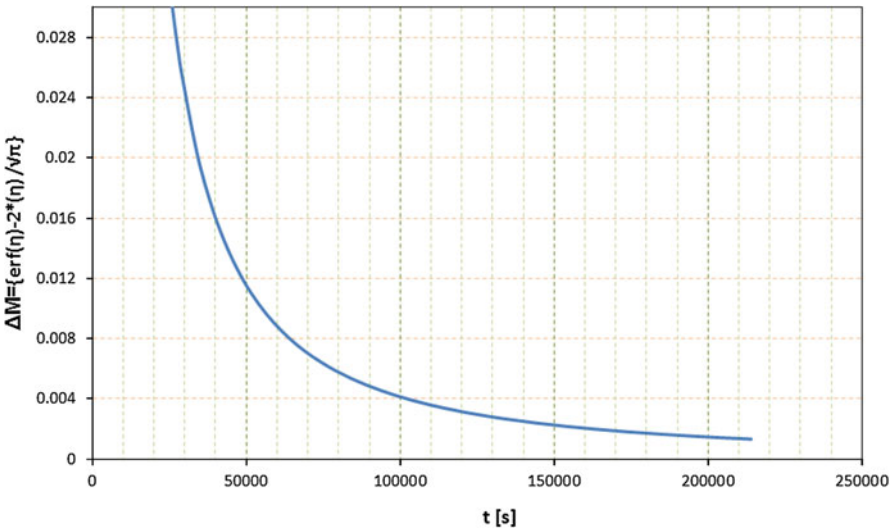

Fig. 4 Function ΔM versus time

Such that

$$\Delta M = \left\{ erf\,(x) - \frac{2}{\sqrt{\pi}}\,(x) \right\}$$

Or, in other words, the difference between the complementary error function and the first term of the series expansion, assuming that $\dot{Q} = 40$ [W], r = 0.15 m, and k = 0.5. It was found that for times greater than 35,000 s, the error ΔM made when considering only the first term of the sum instead of the entire sum is less that 2 %.

Figure 4 shows the function ΔM versus time.

In this situation we obtain the integrals $\int_0^{R_{ext}} T\,(r, t) \cdot r^2 \cdot dr$ and $\int_0^t T\,(R_{ext}, t) \cdot dt$ that appear in Eq. 5. On the one hand:

$$\int_0^{R_{ext}} T\,(r,t) \cdot r^2 \cdot dr = \int_0^{R_{ext}} \frac{\dot{Q} \cdot r^2}{4 \cdot \pi \cdot r \cdot k} \cdot \left(1 - \frac{2}{\sqrt{\pi}} \cdot \frac{r}{2 \cdot \sqrt{\alpha \cdot t}}\right) \cdot dr$$

$$= \frac{\dot{Q}}{24 \cdot \pi \cdot k \cdot (\pi \cdot \alpha)^{1/2} \cdot t^{1/2}} \cdot \left(3 \cdot (\pi \cdot \alpha)^{1/2} \cdot t^{1/2} \cdot R_{ext}^2 - 2 \cdot R_{ext}^3\right)$$

And on the other, by making $r = R_{ext}$, it follows that:

$$T\,(R_{ext}, t) = \frac{\dot{Q}}{4 \cdot \pi \cdot R_{ext} \cdot k \cdot (\pi \cdot \alpha)^{1/2} \cdot t^{1/2}} \cdot \left((\pi \cdot \alpha)^{1/2} \cdot t^{1/2} - R_{ext}\right)$$

We find that:

$$\int_0^t T(R_{ext},t)\cdot dt = \frac{\dot{Q}\cdot(\pi\cdot\alpha)^{1/2}\cdot t - 8\cdot R_{ext}^2\cdot\pi\cdot k\cdot(\pi\cdot\alpha)^{1/2}\cdot t^{1/2}}{4\cdot\pi\cdot R_{ext}\cdot k\cdot(\pi\cdot\alpha)^{1/2}}$$

Substituting and simplifying we are left with:

$$(\rho C_p)^* = (\rho C_p) + \frac{\varsigma\cdot t^{3/2} - \sigma\cdot t}{\chi\cdot t^{1/2} - \omega} \tag{12}$$

where:

$$\begin{aligned}\varsigma &= 6\cdot\dot{Q}\cdot h\cdot S_R\cdot(\pi\cdot\alpha)^{1/2}\\ \sigma &= 8\cdot R_{ext}^2\cdot h\cdot S_R\cdot\pi\cdot k\cdot(\pi\cdot\alpha)^{1/2}\\ \chi &= 12\cdot\dot{Q}\cdot\pi\cdot(\pi\cdot\alpha)^{1/2}\cdot R_{ext}^3\\ \omega &= 8\cdot\pi\cdot\dot{Q}\cdot R_{ext}^4\end{aligned}$$

This means that the auxiliary function $(\rho C_p)^*$ which we procured using the model, and calculated based on the tests, is the sum of (ρC_p) and another time-dependent term. This function has a singularity for time $t = (\omega/\chi)^2 = \left(\frac{2\cdot R_{ext}}{3\cdot(\pi\cdot\alpha)^{1/2}}\right)^2$ s. If we make $R_{ext} = 0.24$ m and assume that $\alpha = 0.045e-5$, then we find that the singularity corresponds to a time period of 18,000 s outside the field of approximation used above. This means that in non-steady state, for values of $t > 35{,}000$ s, the parameter $(\rho C_p)^*$ is approximately the sum of a constant value, (ρC_p), plus an additional term that represents a straight line with slope ς/χ.

We confirm that:

$$\lim_{t\to 0}(\rho C_p)^* = (\rho C_p)$$

Once can thus determine the value of (ρC_p) as the value where the straight segment of the experiment's curve from Fig. 4 meets the y-axis, disregarding all times lower than 35,000 s.

First, in an Excel spreadsheet, the values of a_i, b_i and c_i are determined. Next, for each time, $(\rho C_p)^*$ is determined based on the equation [5]. Table 3 shows an example of the result of calculating $(\rho C_p)^*$ for different times in one of the tests with sand.

The values are graphed using $t - (\rho C_p)^*$, and the values for $t \le 35{,}000$ are eliminated, along with the steady state values. A linear regression is made and the Y-intercept of the line is the value of (ρC_p).

Figure 5 shows $(\rho C_p)^* - t$ for the same test as in Table 3.

Disregarding the results from times less than 35,000 s, the values of $(\rho C_p)^*$ given by Eq. 11 were used to perform a regression, using the program MATLAB. This provided us with the adjustment results shown in Table 4.

Table 3 Example of how $(\rho C_p)^*$ was determined for different times in test 4 of the sand sample

t (s)	T_{1t}	T_{2t}	T_{3t}	T_{4t}	T_{5t}	T_{6t}	$(\rho C_p)^*$
120	0.088	0.096	0.113	0.162	0.113	0.085	1,717,044
180	0.069	0.089	0.098	0.155	0.092	0.073	3,206,181
240	0.126	0.103	0.114	0.17	0.112	0.089	3,367,059
300	0.242	0.119	0.118	0.171	0.115	0.088	4,075,012
360	0.43	0.151	0.11	0.165	0.109	0.079	5,514,246

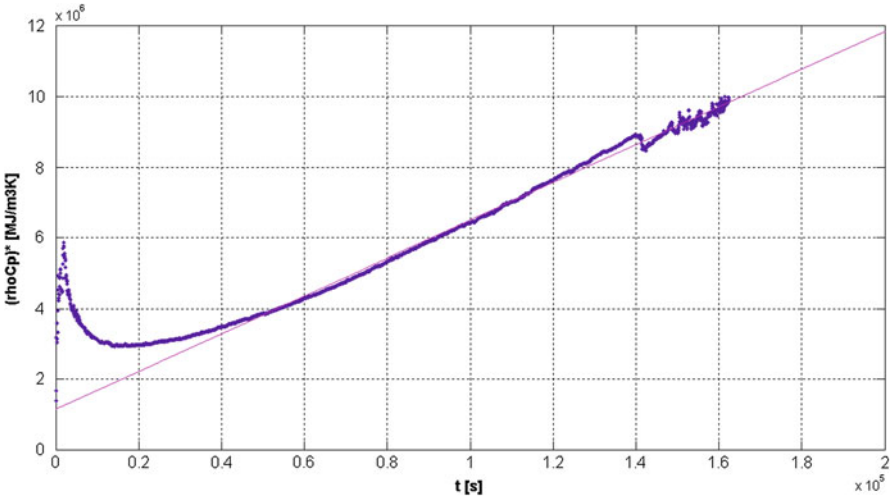

Fig. 5 Adjustment with the Matlab of ρC_p for test 4 (sand) excluding the first 35,000 s, and the maximum time proportional to ρC_p expected, i.e, more than 100,000 s

Table 4 Result of MATLAB's curve fitting tools for sand test 4

General model:	
$(\rho C_p)^* = (\rho C_p) + \varsigma/\chi \cdot t$	
Coefficients (with 95 % confidence bounds):	
$\varsigma/\chi =$	44.33 (44.19, 44.47)
$\rho C_p =$	1.618e+006 (1.608e+006, 1.628e+006)
Goodness of fit:	
SSE:	2.096e+012
R-square:	0.9972
Adjusted R-square:	0.9972
RMSE:	4.403e+004

Table 5 Results of the experimental calculations and the calculation of the cuttings' volumetric heat capacity ρC_p

Experiment	Clay	Sand	Limestone	Shale
ρC_p				
1	1.17	1.41	1.193	1.375
2	1.31	1.43	1.361	0.9131
3	1.19	1.56	1.23	0.9896
4	1.31	1.62		
5	1.27	1.50		
Average	1.25	1.50	1.26	1.09

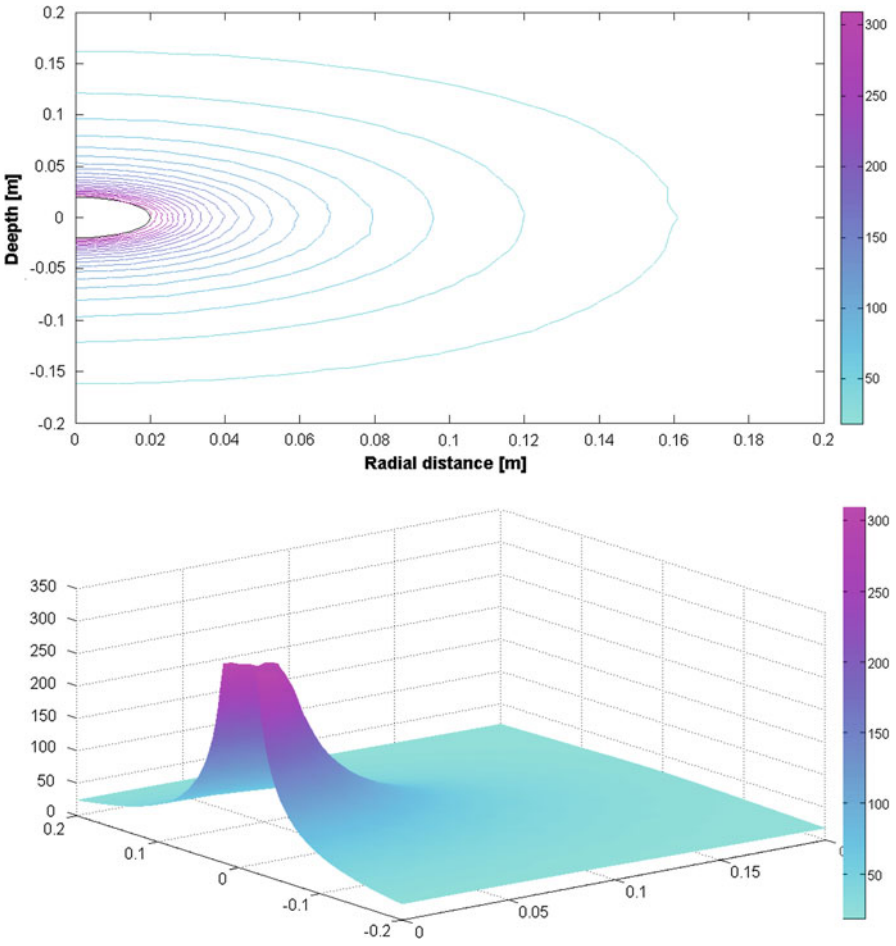

Fig. 6 Result of the simulation with the Matlab program in clay tests

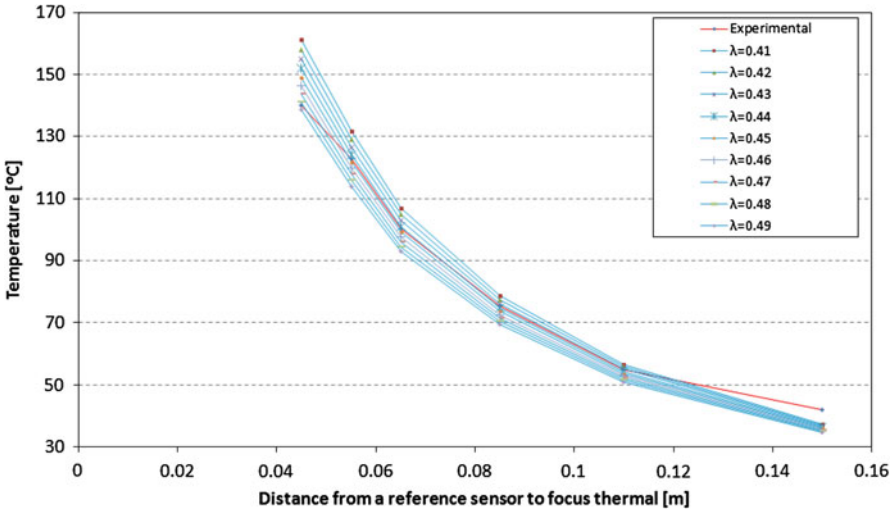

Fig. 7 Profile of temperatures in the sensors line, according to the temperature experimental measurements and according to simulation carried out with the Matlab program for the conductivity values between 0.41 and 0.49

As a result of the experiments and adjustments, the following values were obtained for ρC_p for the samples in question (Table 5).

6 Confirming the validity of the model

To confirm whether or not the simplifications applied in devising the model were indeed valid, we conducted a simulation using MATLAB. We used the experimental geometry, and entered the values for the heat source and the thermal parameters of the ground that we obtained in the experiments with the clays. We then calculated the temperatures of the different sensors. As a result of this simulation we obtained the results in graph form that are shown in the Fig. 6.

The Fig. 7 shows a temperature profile in steady-state conditions for the different sensors, as well as the results of the simulation for the material's thermal conductivity between the different values obtained for the experiment, namely 0.41 and 0.49 W/mK. This confirmed that the temperatures found in the experiment (in red on the graph) match up perfectly with a conductivity of 0.45 W/mK. Furthermore, it confirms that the deviations that occur in the sensors that are farthest away from the heat source are due to the fact that, in these points, the model deviates from reality, as was predicted and indicated in the hypotheses.

7 Conclusions

1. The procedure proposed in this paper makes it possible to assess the thermal properties of borehole cuttings using a simple and inexpensive laboratory method.
2. This method produces values that reflect the real and repeated values obtained in the different tests, in spite of the approximations used.

3. A possible disadvantage of this procedure is that it uses large ground samples, and in boreholes that cut through narrow lithological layers, cuttings from each layer may not be large enough to satisfy the initial hypotheses.
4. The period during which measurements are taken, until steady-state conditions are reached, is relatively long.
5. The conductivity calculation is relatively easy to do because it is determined in steady-state conditions.
6. There are several drawbacks related to the fact that volumetric heat capacity must be calculated during non-steady-state conditions. A number of elements must be simplified, such as the complementary error function, which is linearised.
7. Given the validation of the conductivity results through numerical procedures, along with the conformity of the hypotheses to the experiment, we may conclude that the proposed experimental model is suitable for determining this parameter. The values found in these experiments with cuttings are lower than the corresponding values indicated in the literature for the lithologies of origin. This is due to the fact that, in cuttings, the heat transfer process involves not only conduction through the material itself, but also conduction through air, which would not occur in virgin ground.

Acknowledgments This work has been supported by HUNOSA, the Government of the Principality of Asturias through its Science, Technology and Innovation Scheme, and the University of Oviedo. The authors would like to thank the above-mentioned bodies for their collaboration and financial support during this study.

References

1. K. Horai, G. Simmons, Thermal conductivity of rock-forming minerals. Earth Planet. Sci. Lett. **6**, 359–368 (1969)
2. K. MidttØmme, E. Roalset, P. Aagaard, Thermal conductivities of argillaceous sediments. Geol. Soc. Lond. Eng. Geol. Special Publ. **12**, 355–363 (1997)
3. F. Brigaud, D.S. Chapman, S. Le Douaran, Estimating thermal. Conduct. Sediment. Basins Using Lithol. Data Geophys. Well Logs **74**, 1459–1477 (1990)
4. J.A. Shonder, J.V. Beck, A new method to determine the thermal propierties of soil formations from in situ field tests. Avalaible from http://www.osti.gov/bridge (2000)
5. T. Alonso-Sánchez, M.A. Rey-Ronco, F.J. Carnero-Rodríguez, M.P. Castro-García, Determining ground thermal properties using logs and thermal drill cutting analysis. First relationship with thermal response test in principality of Asturias, Spain. Appl. Therm. Eng. **37**, 226–234 (2012)
6. N.K. Jain, Thesis: *Parameter Estimation of Ground Thermal Properties*. (Oklahoma State University, Stillwater, 1999)
7. H.S Carslaw, J.C. Jaeger, *Conduction of heat in solids* (Claremore Press, Oxford, 1947)
8. L.R. Ingersoll, O.J. Zobel, A.C. Ingersoll, *Heat conduction with engineering and geological application* (McGraw-Hill, New York, 1948)
9. J.D. Deerman, S.P. Kavanaugh, Simulation of vertical U-tube ground-coupled heat pump systems using the cylindrical heat source solution. ASHRAE Trans. **97**, 287–295 (1991)
10. P. Eskilson. Thesis: *Thermal Analysis of Heat Extraction Boreholes* (Department of Mathematical Physics, University of Lund, Sweden, 1987)
11. G. Hellström, B. Sanner. *PC-programs and Modelling for Borehole Heat Exchanger Design*. (International Geothermal Days Germany, Bad Urach, 2001)
12. T. Austin. Thesis: *Development of an In Situ System for Measuring Ground Thermal Properties*, Masters Thesis, (Oklahoma State University, Stillwater, Oklahoma, 1998)